

QCD thermodynamics from lattice calculations with non-equilibrium methods: The SU(3) equation of state

Michele Caselle^{a,b,c}, Alessandro Nada^{a,c,d}, and Marco Panero^{a,c}

^aDepartment of Physics and ^bArnold-Regge Center, University of Turin, and ^cINFN, Turin
Via Pietro Giuria 1, I-10125 Turin, Italy

^dNIC, DESY
Platanenallee 6, D-15738 Zeuthen, Germany

E-mail: caselle@to.infn.it, alessandro.nada@desy.de,
marco.panero@unito.it

Abstract

A precise lattice determination of the equation of state in SU(3) Yang-Mills theory is carried out by means of a simulation algorithm, based on Jarzynski's theorem, that allows one to compute physical quantities in thermodynamic equilibrium, by driving the field configurations of the system out of equilibrium. The physical results and the computational efficiency of the algorithm are compared with other state-of-the-art lattice calculations, and the extension to full QCD with dynamical fermions and to other observables is discussed.

1 Introduction and motivation

The phenomenology of the strong interaction at high temperatures and/or densities remains one of the most interesting (yet somehow elusive) research areas in the physics of elementary particles. As nicely summarized by B. Müller in his lecture at the 2013 Nobel Symposium on LHC Physics [1], the novel state of matter produced in nuclear collisions at LHC and RHIC reveals unique features: it is strongly coupled, but highly relativistic; at high temperature it displays the distinctive collective phenomena of a liquid, whereas at low temperatures it turns into a gas of weakly interacting hadrons; while its shear viscosity η is nearly 18 orders of magnitude larger than the one measured for superfluid helium and even 26 orders of magnitude larger than the one of ultracold atoms [2], the ratio of the shear viscosity over the entropy density s is actually *lower* than for those substances, and close to the fundamental quantum-mechanical bound $1/(4\pi)$ [3]; moreover, it thermalizes in a very short time, close to the limits imposed by causality. Finally, the quark-gluon plasma (QGP) is not simply a “rearrangement” of ordinary nuclear matter: rather, it “creates” its own ground state, in which two characterizing features of the hadronic world, color confinement and dynamical chiral-symmetry breaking, are lost.

At the temperatures reached in present heavy-ion-collision experiments—which, when expressed in natural units $\hbar = c = k_B = 1$, are of the order of hundreds of MeV [4]—the QGP is strongly coupled: this demands a theoretical investigation by non-perturbative tools, and the regularization of quantum chromodynamics (QCD) on a Euclidean lattice [5] is the tool of choice for this purpose. Over the past few years, several physical observables relevant for finite-temperature QCD have been studied on the lattice (see refs. [6] for reviews): one of the most prominent among them is the QCD equation of state [7], which determines the evolution of the Universe shortly after the Big Bang, as well as the evolution of the matter produced in the “little bang” at ultrarelativistic nuclear colliders.

While state-of-the-art results for the QCD equation of state, obtained by different collaborations using slightly different types of lattice discretizations, are now consistent with each other, it is worth remarking that such computations still require large computational power, and the multiple extrapolations to the physical limit are far from trivial. For example, in the standard “integral” method [8], the fact that quantum fluctuations at the lattice cutoff scale induce a strong ultraviolet divergence in the free energy associated with the QCD partition function, implies that bulk quantities at thermal equilibrium, such as the pressure p at a finite temperature T , have to be extracted by subtracting the corresponding quantities evaluated in vacuum, and are encoded in numbers that scale like $O(a^D)$ (a being the lattice spacing, and D the Euclidean spacetime dimension, i.e. four): this constrains the values of a that can be probed in these simulations and, as a consequence, the control over systematic uncertainties affecting the extrapolation to the continuum. Similarly, in simulations with staggered fermions, residual taste-symmetry-breaking effects can have an impact on the extrapolation of the quark masses to the physical limit.

Due to these challenges, in the past few years there has been renovated interest in alternative methods to compute the equation of state. In particular, we would like to mention two recent studies, based upon the gradient flow [9] and on the formulation of the theory in a moving reference frame [10]: both of them have been successfully tested in SU(3) Yang-Mills theory without quarks,

and can be extended to full QCD without major obstructions [11]. The thermal properties of a purely gluonic theory, albeit not relevant for a quantitative comparison with experiments, can reveal important universal features, shared by theories with different gauge symmetry [9, 10, 12–23] and/or in different dimensions [24], and, by virtue of the limited computational power required for their numerical Monte Carlo simulation, provide a useful benchmark for new algorithms.

In this manuscript, we present yet another method to compute the SU(3) equation of state, which is based on Jarzynski’s theorem [25, 26]: as will be discussed in detail in section 2, this theorem encodes an exact relation between the ratio of the partition functions associated with two different ensembles (which, in this case, are defined as those of the theory at two different temperatures) to an exponential average of the work done on the system during a *non-equilibrium transformation* driving it from one ensemble to the other. Jarzynski’s theorem is closely related to a set of powerful mathematical identities in non-equilibrium statistical physics, which have been developed since the 1990’s [27]. A first example of application of Jarzynski’s theorem in numerical simulations of lattice gauge theory was presented in ref. [28], but the technique is quite general and versatile, and can be used for a variety of different lattice QCD problems (at zero or at finite temperature). In section 3, after laying out the setup of our numerical calculations, we report a set of high-precision results for the SU(3) equation of state obtained using this method, along with a detailed discussion of the underlying physics, and with a comparison to studies based on different methods [9, 10, 18]. Section 4 is devoted to a discussion of the computational efficiency of our method and to some concluding remarks. A summary of this work has been reported in ref. [29].

2 Jarzynski’s equality

Jarzynski’s equality [25, 26] is a theorem in statistical mechanics, that relates equilibrium and non-equilibrium quantities.

Consider a classical statistical system, which depends on a set of parameters λ (defined in a space Λ), and let H denote its Hamiltonian, which is a function of the degrees of freedom ϕ . When the system is in thermal equilibrium at temperature T , the partition function, defined as

$$Z = \sum_{\{\phi\}} \exp\left(-\frac{H}{T}\right) \quad (1)$$

(where $\sum_{\{\phi\}}$ denotes the sum over all possible ϕ configurations, and, depending on the nature of ϕ and on the theory, may be a finite or an infinite sum, a multiple integral, or a suitably defined functional integral), is related to the Helmholtz free energy F via $Z = \exp(-F/T)$. In eq. (1), both the partition function and the free energy, like H , are functions of λ . Let λ_{in} and λ_{fin} denote two distinct values of λ in parameter space, and let $Z_{\lambda_{\text{in}}}$ and $Z_{\lambda_{\text{fin}}}$ denote the partition functions of the system in thermodynamic equilibrium, when its parameters take values $\lambda = \lambda_{\text{in}}$ and $\lambda = \lambda_{\text{fin}}$, respectively. For a given physical observable \mathcal{O} , let $\langle \mathcal{O} \rangle_{\lambda}$ denote the statistical average of \mathcal{O} in thermal equilibrium in the ensemble with parameters fixed to λ .

Consider now the situation in which the parameters of the system are varied as a function of time t in a certain interval (which can be either finite or infinite) of extrema t_{in} and t_{fin} , according to some, arbitrary but well-specified, function $\lambda(t)$ (or “protocol” for the parameter evolution), with $\lambda(t_{\text{in}}) = \lambda_{\text{in}}$ and $\lambda(t_{\text{fin}}) = \lambda_{\text{fin}}$. Assume that, starting from an initial equilibrium configuration at $t = t_{\text{in}}$, the parameters are let evolve in time, according to the $\lambda(t)$ function; accordingly, the dynamical variables ϕ respond to the variation in the λ parameters, and themselves evolve in time, spanning a trajectory in the field-configuration space. In general, the configurations at all $t > t_{\text{in}}$ are not thermalized, i.e. the $\lambda(t)$ parameter evolution drives the system out of equilibrium (except when $t_{\text{fin}} - t_{\text{in}}$ is infinite, so that the switching process is infinitely slow). Let W denote the total work done on the system during its evolution from t_{in} to t_{fin} ; since the system is driven out of equilibrium, the mean value of the work \overline{W} obtained by averaging over an ensemble of such transformations, is in general larger than or equal to the free-energy difference $\Delta F = F_{\lambda_{\text{fin}}} - F_{\lambda_{\text{in}}}$ of equilibrium ensembles with parameters $\lambda = \lambda_{\text{in}}$ and $\lambda = \lambda_{\text{fin}}$:

$$\overline{W} \geq \Delta F. \quad (2)$$

Note that $\overline{W} - \Delta F$ is the amount of work dissipated during the parameter switch, which is directly related to the entropy variation, hence the inequality (2) is nothing but an expression of the second law of thermodynamics. Also, when the parameter switch is infinitely slow (i.e. for $\Delta t = t_{\text{fin}} - t_{\text{in}} \rightarrow \infty$) the system remains in thermodynamic equilibrium throughout the switching process, the transformation is reversible, and the equality sign holds.

However, if one considers the *exponential average* of the work, then it is possible to prove that it is directly related to ΔF through the following *equality*:

$$\overline{\exp(-W/T)} = \exp(-\Delta F/T). \quad (3)$$

Eq. (3) is the main statement of Jarzynski’s theorem [25].

Before discussing the proof of eq. (3) for generic Δt , we observe that when $\Delta t \rightarrow \infty$, the equality holds: in this limit, the parameter switch from λ_{in} to λ_{fin} is infinitely slow, the transformation becomes quasi-static, the system remains in equilibrium for the whole duration of the process, so that the work done on the system is equal to

$$W = \int_{\lambda_{\text{in}}}^{\lambda_{\text{fin}}} \left\langle \frac{\partial H}{\partial \lambda} \right\rangle_{\lambda} d\lambda \quad (4)$$

for every trajectory interpolating between the initial and final ensembles. Hence, in this limit one has $\overline{W} = W$. Moreover, in this limit one also has $\overline{W} = \Delta F$, thus the left-hand side of eq. (3) can be written as

$$\overline{\exp(-W/T)} = \exp(-\overline{W}/T) = \exp(-\Delta F/T), \quad (5)$$

and eq. (3) is trivially recovered.

To prove eq. (3) for finite Δt , let us first consider the case in which the system is initially in thermal equilibrium with a heat reservoir at temperature T , but is isolated from it during the switching process from t_{in} to t_{fin} . Then, one can express the average over the ensemble of

trajectories appearing on the left-hand side of eq. (3) in terms of the time-dependent probability density in phase space $\rho = \rho(\phi, t)$. Given that at $t = t_{\text{in}}$ the system is in thermal equilibrium at temperature T , ρ satisfies the initial condition $\rho(\phi, t_{\text{in}}) = \exp[-H_{\lambda(t_{\text{in}})}(\phi)/T] / Z_{\lambda(t_{\text{in}})}$; moreover, since the system is in isolation during the switching process, the time evolution of ρ at $t > t_{\text{in}}$ is given by Liouville's equation $\dot{\rho} = \{H_{\lambda}, \rho\}$, where the quantity appearing on the right-hand side is the Poisson bracket of H_{λ} and ρ . The evolution law expressed by Liouville's equation is fully deterministic, and a one-to-one mapping exists between each configuration at a generic time t and a configuration ϕ_{in} at the initial time $t = t_{\text{in}}$. As a consequence, the work accumulated along a trajectory going through a configuration ϕ at a generic time t is well-defined and equal to

$$w(\phi, t) = H_{\lambda(t)}(\phi) - H_{\lambda(t_{\text{in}})}(\phi_{\text{in}}) = \int_{t_{\text{in}}}^t \frac{\partial H_{\lambda}}{\partial \lambda} \dot{\lambda} d\tau. \quad (6)$$

Thus, the work accumulated during the evolution starting from $t = t_{\text{in}}$ and leading to a final configuration ϕ at $t = t_{\text{fin}}$ is simply $w(\phi, t_{\text{fin}})$, and the average appearing on the left-hand side of eq. (3) can be expressed as

$$\overline{\exp(-W/T)} = \sum_{\{\phi\}} \rho(\phi, t_{\text{fin}}) \exp[-w(\phi, t_{\text{fin}})/T]. \quad (7)$$

Liouville's theorem implies the conservation of the trajectory density in phase space: hence, $\rho(\phi, t_{\text{fin}}) = \rho(\phi_{\text{in}}, t_{\text{in}}) = \exp[-H_{\lambda(t_{\text{in}})}(\phi_{\text{in}})/T] / Z_{\lambda(t_{\text{in}})}$, so that eq. (7) can be rewritten as

$$\begin{aligned} \overline{\exp(-W/T)} &= \frac{1}{Z_{\lambda(t_{\text{in}})}} \sum_{\{\phi\}} \exp\left[-\frac{H_{\lambda(t_{\text{in}})}(\phi_{\text{in}})}{T}\right] \exp\left[-\frac{H_{\lambda(t)}(\phi) - H_{\lambda(t_{\text{in}})}(\phi_{\text{in}})}{T}\right] \\ &= \frac{1}{Z_{\lambda(t_{\text{in}})}} \sum_{\{\phi\}} \exp\left[-\frac{H_{\lambda(t)}(\phi)}{T}\right] = \frac{Z_{\lambda(t_{\text{fin}})}}{Z_{\lambda(t_{\text{in}})}} = \exp(-\Delta F/T). \end{aligned} \quad (8)$$

If the system remains coupled to a heat reservoir during the parameter switch (and the coupling of the system to the reservoir is sufficiently small), then this argument can be repeated for the union of the system and the reservoir, which can be thought of as a larger system, that remains isolated during the process. Then, the work performed on the system equals the difference of the total energy, evaluated on the final and on the initial configuration. This difference does not depend on the switching time, therefore it can be evaluated in the $\Delta t \rightarrow \infty$ limit, in which, as we discussed above, eq. (3) holds. Actually, one can prove that the assumption of weak coupling between the system and the reservoir can be relaxed, if the reservoir is mimicked by a Nosé-Hoover thermostat [30] or a Metropolis algorithm, as is the case in Monte Carlo simulations.

Eq. (3) can also be derived using a master-equation approach, and assuming a completely stochastic (rather than deterministic) evolution for the trajectory [26]: let $P(\phi', t|\phi, t + \Delta t)$ denote the conditional probability of finding a field configuration ϕ at time $t + \Delta t$, given that the system was in configuration ϕ' at time t , and define the instantaneous transition rate from ϕ' to ϕ as

$$R_{\lambda}(\phi', \phi) = \lim_{\Delta t \rightarrow 0^+} \frac{\partial}{\partial(\Delta t)} P(\phi', t|\phi, t + \Delta t). \quad (9)$$

Note that this quantity depends on time only through the time-dependence of λ . Consider now an ensemble of stochastic, Markovian temporal evolutions (or trajectories) of the system, given a certain, fixed time-evolution of its parameters, $\lambda(t)$: the distribution density of these trajectories in phase space $f(\phi, t)$ obeys

$$\frac{\partial}{\partial t} f(\phi, t) = \sum_{\{\phi'\}} f(\phi', t) R_\lambda(\phi', \phi) = \hat{R}_\lambda f, \quad (10)$$

where the last equality is the *definition* of the \hat{R}_λ operator. The formal solution of eq. (10), with the boundary condition that at $t = t_{\text{in}}$ the distribution density equals $f_{\text{in}}(\phi)$, can then be written as

$$f(\phi, t) = \exp \left[(t - t_{\text{in}}) \hat{R}_\lambda \right] f_{\text{in}}(\phi). \quad (11)$$

If λ does not depend on time, then $\phi(t)$ reduces to a standard, stationary Markov process: then, the distribution density $f(\phi, t)$ becomes time-independent and the left-hand side of eq. (10) vanishes. In that case, the Markov process generates an ensemble of configurations distributed according to the canonical Boltzmann distribution for a system with Hamiltonian H_λ at temperature T , i.e. $f(\phi, t) \propto \exp[-H_\lambda(\phi)/T]$, and

$$\sum_{\{\phi'\}} \exp[-H_\lambda(\phi')/T] R_\lambda(\phi', \phi) = 0. \quad (12)$$

Eq. (12) means that the Markov process satisfies detailed balance.¹

Let us assume that the initial distribution at time $t = t_{\text{in}}$ is a canonical one, $f_{\text{in}}(\phi) \propto \exp[-H_{\lambda(t_{\text{in}})}(\phi)/T]$, let $Q(\phi, t)$ denote the average value of $\exp[-w(\phi, t)/T]$ over all trajectories going through a particular configuration ϕ at a generic time t . Introducing the distribution defined as

$$g(\phi, t) = f(\phi, t) Q(\phi, t), \quad (14)$$

the average of $\exp(-W/T)$ over all trajectories can be expressed as

$$\overline{\exp(-W/T)} = \sum_{\{\phi\}} g(\phi, t_{\text{fin}}). \quad (15)$$

From its definition by eq. (14), it is easy to see that the time derivative of g is given by

$$\frac{\partial g}{\partial t} = \frac{\partial f}{\partial t} Q + f \frac{\partial Q}{\partial t} = \hat{R}_\lambda f Q - f \frac{\partial H_\lambda}{\partial \lambda} \frac{\dot{\lambda}}{T} Q = \left(\hat{R}_\lambda - \frac{\partial H_\lambda}{\partial \lambda} \frac{\dot{\lambda}}{T} \right) g. \quad (16)$$

¹One can also assume the stronger condition that, when $t - t_{\text{in}} \rightarrow \infty$, the Markov process always generates a canonical Boltzmann distribution, i.e. that for any, arbitrary, initial distribution $f_{\text{in}}(\phi)$:

$$\lim_{(t-t_{\text{in}}) \rightarrow \infty} \exp \left[(t - t_{\text{in}}) \hat{R}_\lambda \right] f_{\text{in}}(\phi) = \frac{\exp[-H_\lambda(\phi)/T]}{\sum_{\{\phi\}} \exp[-H_\lambda(\phi)/T]}, \quad (13)$$

so that, for sufficiently long times, the Markov process always leads to *thermalization* of any distribution. Note that eq. (13) is stronger than and implies eq. (12). For our present purposes, however, only eq. (12) is needed.

Moreover, eqs. (6) and (14) also imply that, at $t = t_{\text{in}}$:

$$g(\phi, t_{\text{in}}) = f(\phi, t_{\text{in}}) = \frac{\exp[-H_{\lambda(t_{\text{in}})}(\phi)/T]}{\sum_{\{\phi\}} \exp[-H_{\lambda(t_{\text{in}})}(\phi)/T]} = \frac{\exp[-H_{\lambda(t_{\text{in}})}(\phi)/T]}{Z_{\text{in}}}, \quad (17)$$

where we used the fact that the initial distribution is a canonical one.

According to eq. (12), \hat{R}_λ annihilates $\mathcal{N} \exp(-H_\lambda/T)$ (where \mathcal{N} is an arbitrary constant factor), hence:

$$\left(\frac{\partial}{\partial t} - \hat{R}_\lambda + \frac{\partial H_\lambda}{\partial \lambda} \frac{\dot{\lambda}}{T} \right) \mathcal{N} \exp(-H_\lambda/T) = 0, \quad (18)$$

which means that $\mathcal{N} \exp(-H_\lambda/T)$ is solution to eq. (16). The solution consistent with the boundary condition specified by eq. (17) has $\mathcal{N} = 1/Z_{\text{in}}$, so that

$$g(\phi, t) = \frac{\exp[-H_\lambda(t)(\phi)/T]}{Z_{\text{in}}}. \quad (19)$$

Plugging eq. (19), evaluated at $t = t_{\text{fin}}$, into eq. (15), one finally obtains

$$\overline{\exp(-W/T)} = \frac{1}{Z_{\text{in}}} \sum_{\{\phi\}} \exp[-H_{\lambda(t_{\text{fin}})}(\phi)/T] = \frac{Z_{\text{fin}}}{Z_{\text{in}}}, \quad (20)$$

which proves Jarzynski's theorem.

Note that, even though the distribution of ϕ is a canonical one only at $t = t_{\text{in}}$, in the last term of eq. (20) the canonical partition function of the system at the final value of λ appears, and that this equation relates a genuinely out-of-equilibrium quantity (the average appearing in the first term) to a ratio of equilibrium quantities.

This proof of Jarzynski's equality provides a natural way to implement a numerical evaluation of the free-energy difference appearing on the right-hand side of eq. (3) by Monte Carlo simulation:² having defined a parameter evolution $\lambda(t)$, with $t_{\text{in}} \leq t \leq t_{\text{fin}}$, that interpolates between the initial and final ensembles, and starting from a canonical distribution of configurations, one can drive the system out of equilibrium by varying λ as a function of Monte Carlo time, letting the configurations evolve according to any Markov process that satisfies the detailed-balance condition expressed by eq. (12), and compute $\exp(-W/T)$ during this process. The average expressed by the bar notation on the left-hand side of eq. (3) is then obtained by averaging over a sufficiently large number of such trajectories. This is the numerical strategy that we use in this work, in which the Euclidean action S plays the rôle of H/T .

We close this section with a word of caution. The computational efficiency of this method may strongly depend on the properties of the system under consideration: in particular, physical systems with a very large number of degrees of freedom (such as quantum field theories regularized on a spacetime lattice) have sharply peaked statistical distributions, hindering an accurate sampling of the configuration-space regions that contribute mostly to $\overline{\exp(-W/T)}$. If the different values

²A related idea underlies the annealed-importance-sampling technique [31].

of W in different trajectories are much larger than the scale of typical thermal fluctuations (or of typical quantum fluctuations, for lattice simulations of quantum field theory), then $\overline{\exp(-W/T)}$ is dominated by configurations in which the value of W is much smaller than \overline{W} , and an accurate determination of $\overline{\exp(-W/T)}$ may require a prohibitively large number of trajectories. Note, however, that, in the numerical calculation of free-energy differences by eq. (3), there exists a remarkable difference in the rôles of the initial and final ensembles: one assumes that the initial configurations are thermalized, while the field values at all $t > t_{\text{in}}$ (including, in particular, at $t = t_{\text{fin}}$) are out of equilibrium. This asymmetry between the initial and target ensembles implies that, if the Monte Carlo determination of ΔF is biased by effects due to limited statistics, then carrying out the same calculation in the opposite direction will, in general, give a result different from $-\Delta F$. Conversely, verifying that a “direct” and a “reverse” computation give consistent results, provides a powerful test of the correctness of the calculation. This is a test that all results of our present work pass with success.

3 Lattice calculation of the SU(3) equation of state

In this work, we investigate the behavior of QCD at finite temperature, and compute the equation of state via lattice simulations using an algorithm based on Jarzynski’s equality eq. (3).

In particular, we focus on the pure-gluon sector, which captures the main feature of thermal QCD at the qualitative level: the existence of a confining phase at low temperatures, in which the physical states are massive color singlets, and a deconfined phase at high temperatures, in which chromoelectrically charged, light, elementary particles interact with each other through screened, long-range interactions.³ Thermal screening of both electric and magnetic field components is, indeed, a characterizing feature of the deconfined phase of non-Abelian gauge theories, which defines it as a “plasma”. Asymptotic freedom implies that, when the temperature T is very high, the physical coupling g at the scale of thermal excitations, $O(T)$, becomes small; in this limit, chromoelectric fields are screened on distances inversely proportional to gT , while chromomagnetic fields are screened on lengths inversely proportional to g^2T , so that the theory develops a well-defined hierarchy of scales, between “hard” (of the order of T), “soft” (of the order of gT), and “ultra-soft” (of the order of g^2T) modes, and this separation of scales allows for a systematic treatment in terms of effective theories [33–37]. The appearance of the soft and ultra-soft scales is due to the existence of infra-red divergences, which lead to a breakdown of the correspondence between the number of loops in Feynman diagrams and the order in α_s in perturbative calculations [38], and to the intrinsically non-perturbative nature of long-wavelength modes *at all temperatures*. Moreover, for plasma excitations on the energy scale of the deconfinement temperature, the physical coupling

³We also remind the reader of some notable differences between pure-gluon SU(3) Yang-Mills theory and real-world QCD with dynamical quarks. In particular, in the pure-gluon theory, the confining and deconfined phases are separated by a first-order phase transition taking place at a critical temperature T_c which, when converted into physical units, is about 270 MeV. By contrast, in QCD with physical quarks, the change of state from the confining to the deconfined regimes is rather a smooth crossover, taking place at a lower temperature, around 160 MeV. However, it has been recently argued that the pure Yang-Mills dynamics could nevertheless be relevant for certain aspects of the physics of heavy-ion collisions’ experiments [32].

is not very small, so that the deconfined state of matter cannot be reliably modelled as a gas of free partons.

For these reasons, the study of the equation of state of QCD—or of its gluonic sector, that we are focusing on here—close to deconfinement requires non-perturbative techniques. We carry out this study by discretizing the Euclidean action of SU(3) Yang-Mills theory on a hypercubic lattice Λ of spacing a , spatial volume $V = L^3 = (aN_s)^3$ and extent aN_t along the compactified Euclidean-time direction, using the Wilson action [5]

$$S = \beta \sum_{x \in \Lambda} \sum_{0 \leq \mu < \nu \leq 3} \left(1 - \frac{1}{3} \text{Re Tr } U_{\mu\nu}(x) \right), \quad (21)$$

where $\beta = 6/g_0^2$, with g_0 the bare coupling, and

$$U_{\mu\nu}(x) = U_\mu(x) U_\nu(x + a\hat{\mu}) U_\mu^\dagger(x + a\hat{\nu}) U_\nu^\dagger(x). \quad (22)$$

The partition function of the lattice theory is given by

$$Z = \int \prod_{x \in \Lambda} \prod_{\mu=0}^3 dU_\mu(x) \exp[-S(U)] \quad (23)$$

(where $dU_\mu(x)$ is the Haar measure for the SU(N) matrix defined on the oriented link from site x to site $x + a\hat{\mu}$) and expectation values are defined as

$$\langle \mathcal{O} \rangle = \frac{1}{Z} \int \prod_{x \in \Lambda} \prod_{\mu=0}^3 dU_\mu(x) \mathcal{O} \exp[-S(U)]. \quad (24)$$

The integrals on the right-hand side of eq. (24) are estimated numerically, by Monte Carlo integration, from a sample of field configurations produced in a Markov chain; our update algorithm combines one heat-bath [39] and five to ten over-relaxation steps [40] on the link variables of the whole lattice: this defines a “sweep”. The uncertainties in these simulation results are estimated with the jackknife method [41].

The physical temperature of the system $T = 1/(aN_t)$ is varied by varying a , which, in turn, can be continuously tuned by varying β : to this purpose, we set the scale of our lattice simulations by means of the Sommer scale r_0 [42] as determined in [43]. The critical temperature is related to r_0 by $T_c r_0 = 0.7457(45)$ [22].⁴

Our lattice determination of the equation of state rests on the following thermodynamic identity, relating the pressure p to the free energy per unit volume $f = F/V$,

$$p = -f = \frac{T}{V} \ln Z, \quad (25)$$

⁴Note that, if r_0 is assumed to be of the order of 0.5 fm (a figure consistent with phenomenological potential models for QCD), then the critical deconfinement temperature in SU(3) Yang-Mills theory is almost twice as large as in QCD. The fact that deconfinement takes place at lower temperatures for theories with a larger number of colored degrees of freedom in the deconfined phase [14, 20, 44] is consistent with a qualitative argument, based on the mismatch between the number of degrees of freedom at low and at high temperatures (see also ref. [45]).

which holds in the thermodynamic limit, $V \rightarrow \infty$, and receives negligible corrections for the L and T values considered here [16, 46, 47]. Following the algorithmic strategy discussed in ref. [28] for a benchmark study in the SU(2) theory, we study how the dimensionless $p(T)/T^4$ ratio varies as a function of the temperature, starting from an initial temperature T_{in} :

$$\frac{p(T)}{T^4} - \frac{p(T_{\text{in}})}{T_{\text{in}}^4} = \left(\frac{N_t}{N_s}\right)^3 \ln \frac{Z(T)}{Z(T_{\text{in}})}. \quad (26)$$

In our simulations, we compute $Z(T)/Z(T_{\text{in}})$ by means of Jarzynski's equality, using β (by tuning which, as stated above, the temperature can be varied continuously) as the λ parameter: β is let evolve linearly with the Monte Carlo time t between the initial (β_{in}) and final (β_{fin}) values corresponding to T_{in} and T , respectively. More precisely, the β interval is discretized in N equal intervals of width $\Delta\beta$, so that $\beta_n = \beta_{\text{in}} + n(\beta_{\text{fin}} - \beta_{\text{in}})/N = \beta_{\text{in}} + n\Delta\beta$. Finally, one should remember that the $p(T)$ and $p(T_{\text{in}})$ terms appearing on the left-hand side of eq. (26) also include contributions from quantum (non-thermal) fluctuations, that depend on the lattice cutoff and diverge in the continuum limit. These contributions can be removed from p by evaluating the quantity appearing on the right-hand side of eq. (26) on a lattice of large hypervolume $(aN_0)^4$ at $T = 0$ at the same a . This leads us to define the physical, renormalized pressure as

$$\frac{p(T)}{T^4} = \frac{p(T_{\text{in}})}{T_{\text{in}}^4} + \left(\frac{N_t}{N_s}\right)^3 \left[\overline{\ln \exp(-\Delta S_{N_s^3 \times N_t})} - \gamma \overline{\ln \exp(-\Delta S_{N_0^4})} \right], \quad (27)$$

where ΔS is the variation in Euclidean action during a non-equilibrium trajectory in configuration space:

$$\Delta S = \sum_{n=0}^{N-1} \{S[\beta_{n+1}, U(t_n)] - S[\beta_n, U(t_n)]\}, \quad (28)$$

the $N_s^3 \times N_t$ and N_0^4 subscripts respectively indicate that this quantity is evaluated on a finite- or on a zero-temperature lattice, $\gamma = N_s^3 \times N_t / N_0^4$, and the bar denotes the average over a sample of n_{traj} non-equilibrium trajectories, which start from canonically distributed initial configurations $\{U(t_0)\}$. Note that the summands on the right-hand side of eq. (28) are given by the action difference induced by a variation of β on the same field configuration. In practice, in order to scan a wide temperature range, from the confining to the deconfined phase, it is more convenient to divide the temperature interval in a number (that we denote as n_{int}) of smaller intervals. In particular, we choose these intervals in such a way that they do not stretch across different phases: this allows us to get rid of potential difficulties that might arise in the numerical sampling of configurations, when the algorithm tries to probe the physics at $T > T_c$, by driving configurations in the $T < T_c$ phase out of equilibrium, without letting them thermalize.⁵ Dividing the β range of interest in a different number of intervals that do not cross the phase transition should lead to

⁵A different computational strategy, that would allow the algorithm to avoid the critical point, consists in deforming the action by adding operators that could turn the deconfinement transition into a crossover (e.g. traces of Wilson lines in the Euclidean-time direction), and varying their coefficients to turn them on only near the critical temperature. This numerical strategy, however, is more complex, and we did not explore it in the present work.

the same physical results, but n_{int} has some effect on the numerical efficiency of the simulation algorithm. In particular, smaller values of n_{int} (i.e. broader intervals in β) typically require larger values of N and more statistics. On the other hand, larger n_{int} implies a larger overhead for thermalization of the initial configurations at the start of each transformation (in this work we used 5000 full thermalization sweeps at $T = 0$ and 15000 at finite temperature).

We run our simulations on lattices with $N_t = 6, 7, 8$ and 10 and for $N_s > 12N_t$ (and typically $N_s \simeq 16N_t$), according to the parameters listed in table 1, where $n_{\text{traj}} = 10$ throughout, and n_{conf} denotes the total number of configurations used for each combination of parameters, given by the sum of the $N \cdot n_{\text{traj}}$ products over all n_{int} intervals.

N_t	N_s	N_0	β range	temperature range	n_{int}	n_{conf}	$\Delta\beta$
6	96	48	[5.72785, 5.89985]	$[0.7T_c, T_c]$	3	1.7×10^5	$10^{-5} - 2 \times 10^{-5}$
6	96	48	[5.89985, 6.50667]	$[T_c, 2.5T_c]$	6	3.7×10^5	$10^{-5} - 2 \times 10^{-5}$
7	112	48	[5.79884, 5.98401]	$[0.7T_c, T_c]$	3	2.4×10^5	10^{-5}
7	112	48	[5.98401, 6.6279]	$[T_c, 2.5T_c]$	4	3.3×10^5	$10^{-5} - 2 \times 10^{-5}$
8	120	48	[5.86415, 6.06265]	$[0.7T_c, T_c]$	3	2.6×10^5	$10^{-5} - 2 \times 10^{-5}$
8	120	48	[6.06265, 6.72223]	$[T_c, 2.5T_c]$	9	1.2×10^5	$10^{-5} - 8 \times 10^{-5}$
10	120	48	[5.98408, 6.2068]	$[0.7T_c, T_c]$	5	3.1×10^5	$7.5 \times 10^{-6} - 10^{-5}$
10	160	48	[6.2068, 6.9033]	$[T_c, 2.5T_c]$	8	1.3×10^5	$10^{-5} - 10^{-4}$

Table 1: Parameters of our simulations.

The pressure p is the primary thermodynamic observable that we compute using Jarzynski's equality, according to eq. (27): the results at the different values of N_t are shown in fig. 1.

From the results for p/T^4 at finite lattice spacing, we take the continuum limit by first interpolating them, for each N_t , through cubic splines, and then by fitting the splines at fixed values of T with a constant-plus-linear-term fit in $1/N_t^2$:

$$p_{N_t}(T) = \alpha(T) + \frac{\beta(T)}{N_t^2}. \quad (29)$$

This defines $\alpha(T)$ as the continuum-extrapolated value of the pressure at that temperature. Different types of interpolations at fixed N_t , or more complicated functional forms than the one in eq. (29), yield compatible results. As the starting value for p/T^4 at $T_{\text{in}} = 0.7T_c$, we use $p(T_{\text{in}})/T_{\text{in}}^4 = 0.00086$, the analytical result for a glueball gas [48] (for a thorough discussion, see also refs. [49] and references therein). Our results for p/T^4 obtained in this way are shown in figure 2, in comparison with those from refs. [10, 18].

Other basic thermodynamic observables, like the trace of the energy-momentum tensor Δ , the energy per unit volume ϵ , and the entropy per unit volume s are directly related to the pressure

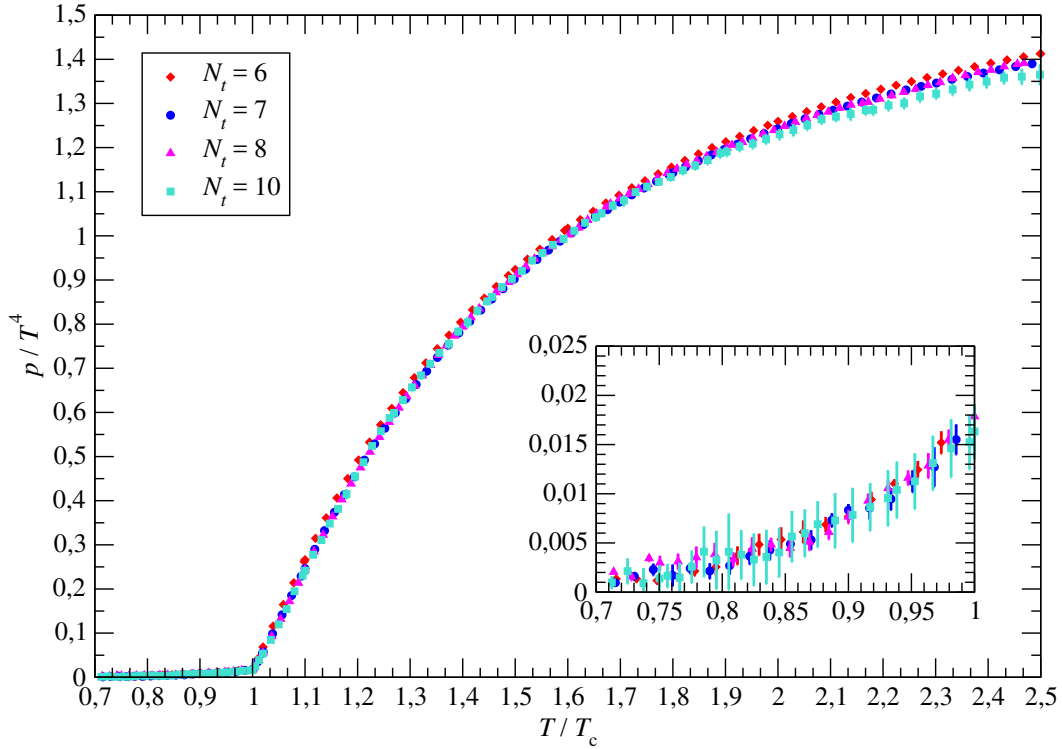


Figure 1: Results for p/T^4 , as a function of T/T_c , from simulations at different values of N_t . The inset shows a zoom onto the confining phase, $T < T_c$.

by basic thermodynamic relations:

$$\Delta = T^5 \frac{\partial}{\partial T} \left(\frac{p}{T^4} \right), \quad (30)$$

$$\epsilon = \frac{T^2}{V} \frac{\partial}{\partial T} \ln Z = 3p + \Delta, \quad (31)$$

$$s = \frac{\ln Z}{V} + \frac{\epsilon}{T} = \frac{4p + \Delta}{T}. \quad (32)$$

To compute the trace of the energy-momentum tensor, we first fit our continuum values for

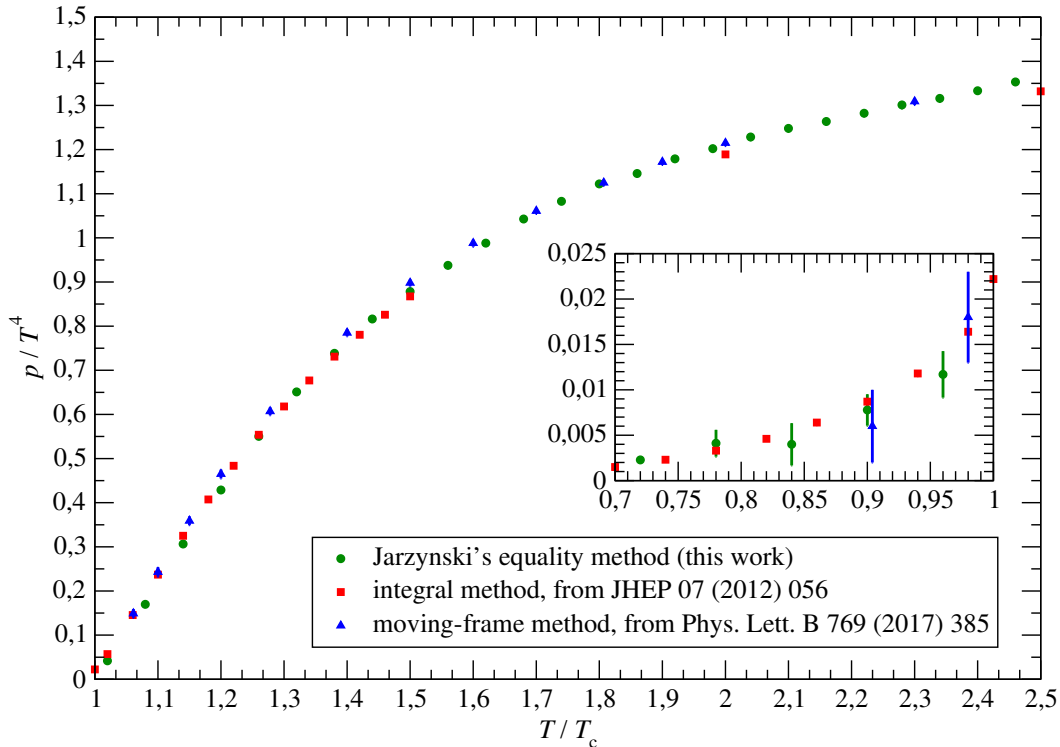


Figure 2: Our results for p/T^4 , extrapolated to the continuum (green circles), as a function of T/T_c , in comparison with those obtained with the integral method in ref. [18] (red squares) and with those obtained using the moving-frame method in ref. [10] (blue triangles). The results in the confining phase are displayed in the inset plot.

p/T^4 in the temperature range $T_c \leq T \leq 2.5T_c$, to the following rational function of $w = \ln(T/T_c)$:

$$\frac{p}{T^4} = \frac{p_1 + p_2 w + p_3 w^2}{1 + p_4 w + p_5 w^2}. \quad (33)$$

The fit gives $p_1 = 0.0045(35)$, $p_2 = 1.76(12)$, $p_3 = 10.6(2.2)$, $p_4 = 2.07(47)$, and $p_5 = 5.8(1.1)$, with a reduced χ^2 equal to 0.33. Deriving the function on the right-hand side of eq. (33), we obtain the results for the trace of the energy-momentum tensor shown in fig. 3, where we compare them with those that have been recently obtained by different groups, using other methods [9, 10, 18].

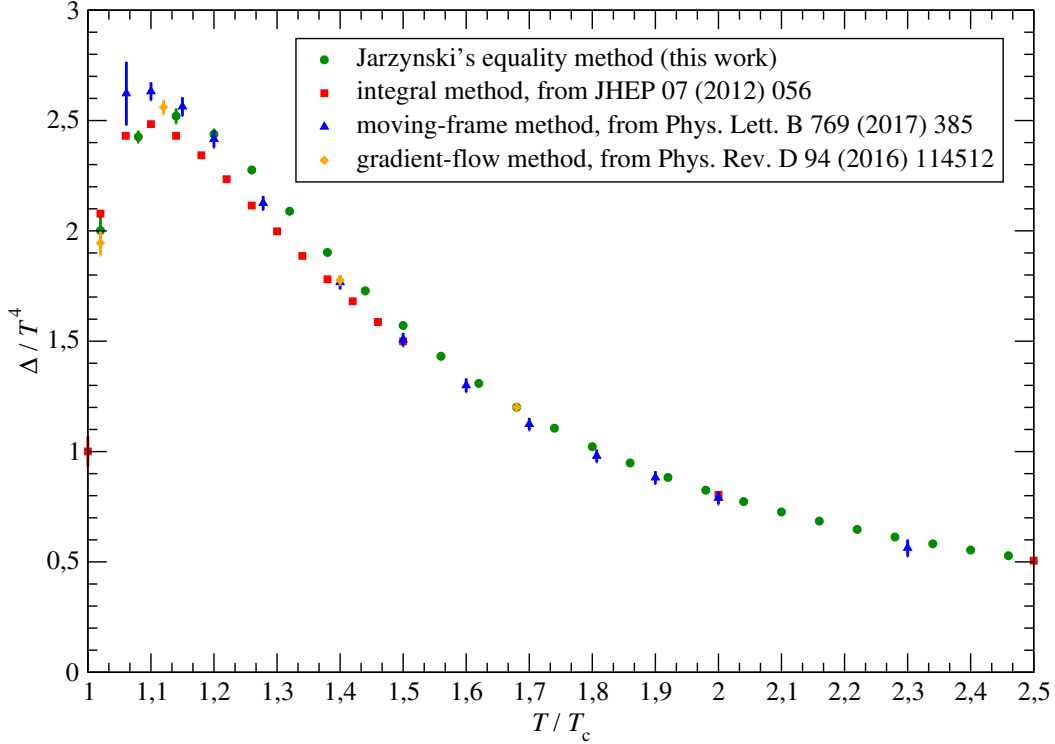


Figure 3: Our continuum-extrapolated results for Δ/T^4 (green circles), as a function of T/T_c , in comparison with those obtained with the integral method in ref. [18] (red squares), with those obtained using the moving-frame method in ref. [10] (blue triangles), and with those computed using the gradient-flow method in ref. [9] (orange diamonds).

Finally, the energy density and the entropy density are simply obtained using eq. (31) and eq. (32), respectively: the results are shown in figs. 4 and 5.

The complete set of our continuum-extrapolated results for p/T^4 , Δ/T^4 , ϵ/T^4 , and s/T^3 is reported in table 2.

4 Discussion and concluding remarks

The results presented in section 3 deserve several relevant comments.

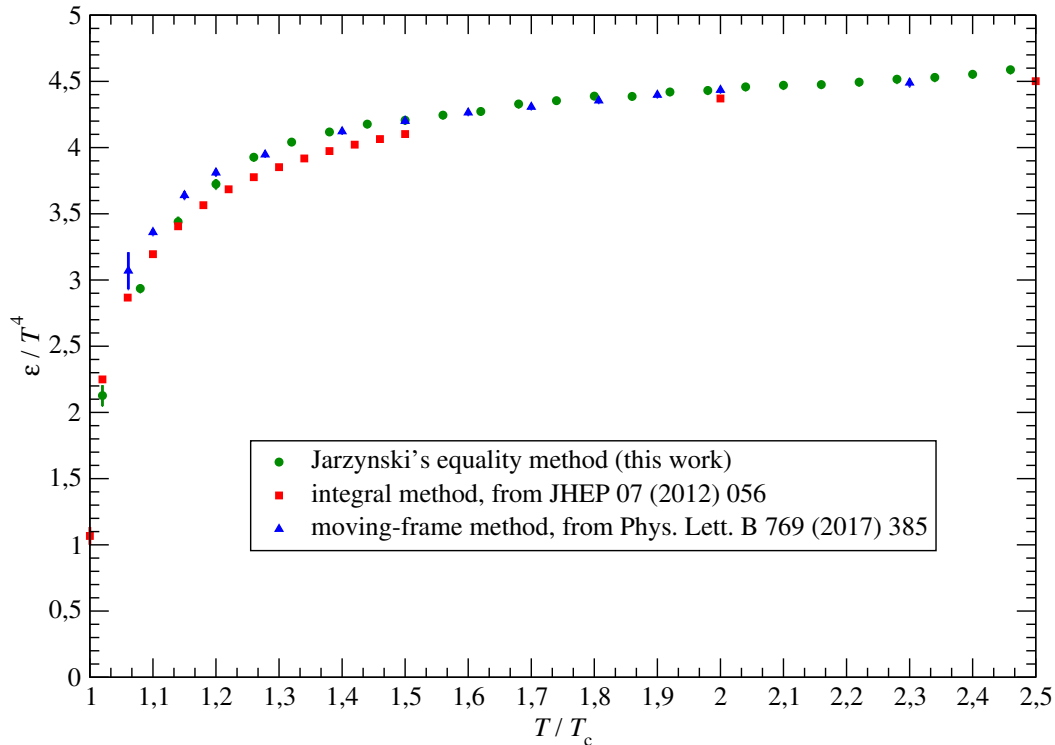


Figure 4: Same as in fig. 2, but for the energy density in units of the fourth power of the temperature.

First and foremost, the comparison of our data, obtained with an algorithm based on Jarzynski's equality, with those from previous works [9, 10, 18] provides a striking check of the expected universality of lattice results: the fact that the high-precision results obtained by four independent groups, using remarkably different computational strategies, are essentially compatible with each other, indicates that all sources of systematic or statistical uncertainties are under control, and confirms that lattice calculations provide solid, first-principle results for the thermodynamics of strong interactions in the temperature range probed by heavy-ion collision experiments. Looking at the fine details, however, one can also see that some slight tension between the results obtained with different methods still persists. For example, the results for the various thermodynamic observables reported in ref. [18] appear to be systematically lower than the others. This effect is

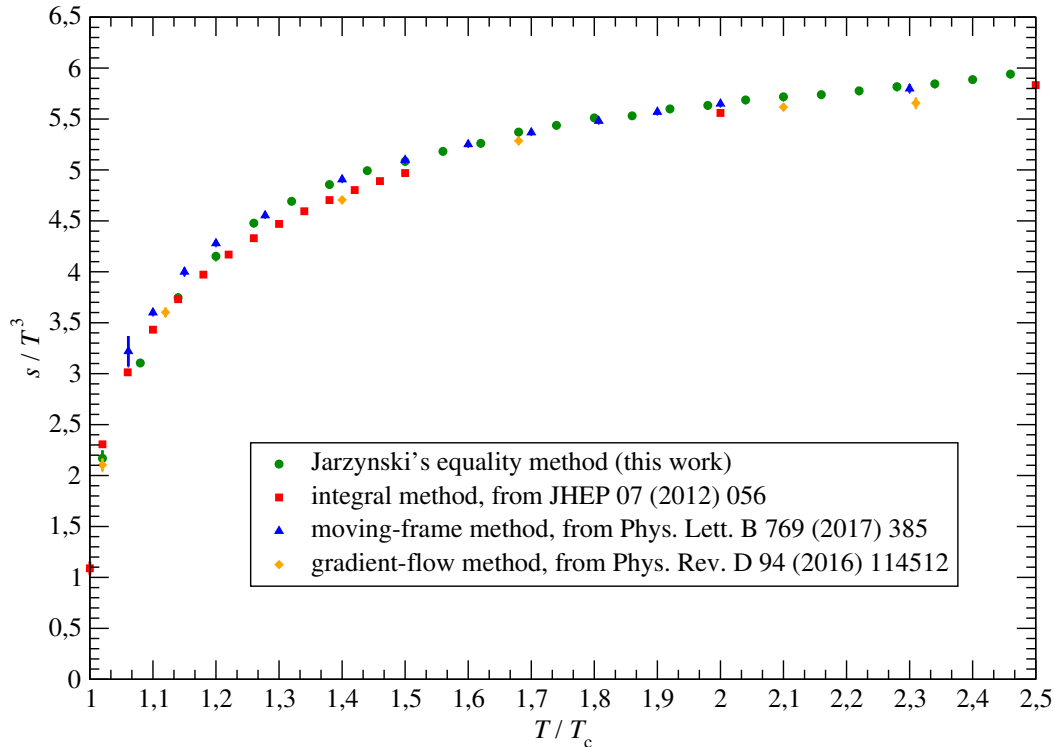


Figure 5: Same as in fig. 3, but for the entropy density in units of the third power of the temperature.

most visible for the trace of the energy momentum tensor in figure 3, while it is essentially absent in the results for the pressure shown in figure 2 (whereas the energy and entropy densities, being obtained from linear combinations of p and Δ , exhibit an intermediate behavior, with milder tensions). Also, the discrepancy appears to be largest in the temperature region of the peak in Δ/T^4 , where it is comparable (in sign and magnitude) with the difference from the results from ref. [12] that was reported in ref. [18] itself. While the origin of this slight difference between the results of ref. [18] and the others remains unclear, it should be remarked that it is quantitatively modest, and does not change the overall physical picture of the SU(3) equation of state in a significant way.

In terms of physics, these results confirm that, in the temperature range relevant for collider

T/T_c	p/T^4	Δ/T^4	ϵ/T^4	s/T^3
0.72	0.0023(3)	0.0137(38)	0.021(17)	0.023(17)
0.78	0.0041(15)	0.0200(57)	0.032(20)	0.036(21)
0.84	0.0040(23)	0.0286(87)	0.041(23)	0.045(25)
0.90	0.0078(17)	0.044(14)	0.067(24)	0.075(26)
0.96	0.0117(26)	0.072(23)	0.107(32)	0.119(35)
1.02	0.0418(28)	2.001(78)	2.127(78)	2.169(79)
1.08	0.1698(32)	2.426(27)	2.936(30)	3.106(32)
1.14	0.3064(42)	2.520(34)	3.439(39)	3.746(41)
1.20	0.429(6)	2.438(25)	3.724(38)	4.153(43)
1.26	0.550(5)	2.276(16)	3.927(27)	4.477(32)
1.32	0.651(5)	2.089(14)	4.041(23)	4.693(27)
1.38	0.739(5)	1.902(15)	4.118(22)	4.856(26)
1.44	0.816(7)	1.728(16)	4.177(24)	4.993(30)
1.50	0.878(6)	1.571(16)	4.206(27)	5.084(32)
1.56	0.938(7)	1.432(15)	4.245(26)	5.182(31)
1.62	0.988(7)	1.309(14)	4.273(26)	5.261(31)
1.68	1.043(7)	1.201(12)	4.329(27)	5.372(34)
1.74	1.083(6)	1.106(10)	4.355(25)	5.437(30)
1.80	1.122(6)	1.022(9)	4.389(25)	5.511(31)
1.86	1.146(6)	0.949(8)	4.386(24)	5.532(30)
1.92	1.179(7)	0.883(8)	4.420(25)	5.599(32)
1.98	1.202(8)	0.825(8)	4.431(27)	5.633(35)
2.04	1.229(8)	0.773(8)	4.459(28)	5.687(35)
2.10	1.248(8)	0.727(9)	4.471(29)	5.719(37)
2.16	1.264(8)	0.685(9)	4.476(27)	5.739(34)
2.22	1.282(7)	0.647(10)	4.494(27)	5.776(34)
2.28	1.301(8)	0.613(11)	4.516(30)	5.817(37)
2.34	1.316(8)	0.582(11)	4.530(29)	5.846(37)
2.40	1.333(7)	0.554(12)	4.554(26)	5.887(33)
2.46	1.353(7)	0.528(12)	4.588(28)	5.941(35)

Table 2: Our final, continuum-extrapolated results for the pressure (second column), for the trace of the energy-momentum tensor (third column), and for the energy density (fourth column) in units of the fourth power of the temperature, and for the entropy density in units of the third power of the temperature (fifth column), as a function of the temperature in units of the deconfinement temperature (first column).

experiments, the thermodynamics of SU(3) Yang-Mills theory is dominated by non-perturbative effects, and far from the ideal limit of a gas of free gluons. In particular, the equilibrium observables

considered here are significantly different from their Stefan-Boltzmann values:

$$\frac{p_{\text{SB}}}{T^4} = \frac{8\pi^2}{45}, \quad \frac{\Delta_{\text{SB}}}{T^4} = 0, \quad \frac{\epsilon_{\text{SB}}}{T^4} = \frac{8\pi^2}{15}, \quad \frac{s_{\text{SB}}}{T^3} = \frac{32\pi^2}{45}, \quad (34)$$

which are reached only in the $T \rightarrow \infty$ limit, and approached logarithmically slowly as the temperature is increased. A way to study the values for these quantities at high, but finite, temperatures, is by means of thermal perturbation theory. Weak-coupling expansions for the pressure of QCD (and pure-gluon Yang-Mills theory) have a long history: the leading-order correction, $O(g^2)$, was worked out forty years ago [50]. Soon thereafter, however, it was realized that perturbative expansions in thermal non-Abelian gauge theories have non-trivial features: in particular, the existence of infrared divergences, which have to be resummed, leads to the appearance of terms proportional to *odd* powers and/or logarithms of g , and, most importantly, implies that, at some finite order, an *infinite* number of Feynman diagrams, of *arbitrarily complicated topologies*, will contribute [38]. This ‘‘Linde problem’’ leads to the peculiar situation, in which the number of sensible perturbative orders is finite. For the pressure, this problem occurs at $O(g^6)$, or four loops, and the program of computing all perturbative contributions up to that order has been completed, with the determination of all terms $O(g^3)$ [51], $O(g^4 \ln g)$ [52], $O(g^4)$ [53], $O(g^5)$ [54], and finally $O(g^6 \ln g)$ [37, 55], but the convergence of the perturbative series is known to be very slow [35, 56].

As we already mentioned above, dimensional reduction provides an elegant way to systematically account for the non-perturbative physics related to infrared divergences, by means of effective theories [33] that can be studied non-perturbatively on the lattice [57] (an approach that has recently found useful applications even for real-time phenomena in hot QCD [58]).

The limited convergence of weak-coupling expansions for thermodynamic quantities in finite-temperature QCD is due to the fact that characteristic phenomena of plasmas, such as screening and Landau damping, must be properly accounted for. To this purpose, one can re-arrange the perturbative expansions using a hard-thermal-loop approach [59] (in which, however, the Debye mass m_D in the ‘‘improvement term’’ added to the Lagrangian is, in principle, arbitrary, and must be fixed in a self-consistent way).

In any case, the intrinsically non-perturbative nature of the physics of high-temperature non-Abelian gauge theories makes it hardly surprising that leading-order weak-coupling expansions provide an unsatisfactory description for the equation of state of strong interactions, even at high temperatures. While various phenomenological models (including bottom-up models based on the gauge-gravity duality [60]) describe well the thermodynamics of the quark-gluon plasma at temperatures close to deconfinement [61], lattice calculations remain the most reliable first-principle theoretical tool to study thermal QCD under the conditions probed in heavy-ion collisions.

In this work, we showed that the computational strategy proposed in ref. [28] and based on Jarzynski’s equality [25, 26] provides a robust and efficient tool to compute the equation of state non-perturbatively on the lattice. As we mentioned above, its implementation in Monte Carlo calculations only requires that the Markov process satisfies detailed balance, and the assumption that the initial starting configurations (not those at subsequent Monte Carlo times) are thermalized. Its computational efficiency, which can be tested by checking the mutual consistency of results obtained when the algorithm is run in the direct (from λ_{in} to λ_{fin}) and in the reverse ($\lambda_{\text{fin}} \rightarrow \lambda_{\text{in}}$)

direction, depends crucially on the typical amplitude of fluctuations in W/T (or, in the present context, in Euclidean action) from one trajectory to another. If such fluctuation amplitude (which is an *extensive* quantity) is very large, then the numerical evaluation of the exponential average appearing on the left-hand side of eq. (3) requires a prohibitively large number of trajectories; on the other hand, for moderate fluctuations, the algorithm can estimate the exponential average of $-W/T$ very efficiently, and therefore provide accurate results for the free-energy difference appearing on the right-hand side of eq. (3) at a limited computational cost. The N parameter introduced in section 3, which controls “how violently” the configurations are driven out of equilibrium, plays therefore a key rôle in this respect. Note, in particular, that for $N \rightarrow \infty$ (the “quasi-static limit”) the field configurations remain in equilibrium throughout their evolution from the initial to the final ensemble. Conversely, in the opposite limit (that is, for $N = 1$), our algorithm reduces to the reweighting method [62]. For a detailed discussion of the computational efficiency of algorithms based on Jarzynski’s equality, see also refs. [63].

Extending our algorithm to calculations including dynamical quark flavors is straightforward, and we plan to implement it in code for lattice simulations in full QCD simulations in future work. In this respect, it would be interesting to compare the efficiency of this algorithm to different calculations of the QCD equation of state [7, 11, 64, 65].

Another direction, in which the present work can be generalized, consists in applying the Jarzynski’s equality to lattice calculations of different physical observables. The computational strategy based on this algorithm, indeed, is quite general and versatile, and not restricted to the thermodynamics domain. As a benchmark study, a determination of the interface free energy was presented in ref. [28]; the extension to other quantities, like the running coupling of the strong interaction in the Schrödinger-functional scheme [66] and the entanglement entropy in lattice gauge theory [67], is under way.

Acknowledgements

The simulations were run on the supercomputers of the Consorzio Interuniversitario per il Calcolo Automatico dell’Italia Nord Orientale (CINECA). We thank Martin Hasenbusch, Michele Pepe, and Rainer Sommer for helpful comments and discussions.

References

- [1] B. Müller, (2013), 1309.7616.
- [2] T. Schäfer and D. Teaney, Rept. Prog. Phys. **72**, 126001 (2009), 0904.3107.
- [3] G. Policastro, D. Son, and A. Starinets, Phys. Rev. Lett. **87**, 081601 (2001), hep-th/0104066.
- [4] P. Braun-Munzinger, V. Koch, T. Schäfer, and J. Stachel, Phys. Rept. **621**, 76 (2016), 1510.00442.
- [5] K. G. Wilson, Phys. Rev. **D10**, 2445 (1974).

- [6] O. Philipsen, Prog. Part. Nucl. Phys. **70**, 55 (2013), 1207.5999. H.-T. Ding, F. Karsch, and S. Mukherjee, (2015), 1504.05274. H. B. Meyer, PoS **Lattice 2015**, 014 (2016), 1512.06634.
- [7] S. Borsányi *et al.*, Phys. Lett. **B730**, 99 (2014), 1309.5258. HotQCD, A. Bazavov *et al.*, Phys. Rev. **D90**, 094503 (2014), 1407.6387.
- [8] J. Engels, J. Fingberg, F. Karsch, D. Miller, and M. Weber, Phys. Lett. **B252**, 625 (1990).
- [9] M. Kitazawa, T. Iritani, M. Asakawa, T. Hatsuda, and H. Suzuki, Phys. Rev. **D94**, 114512 (2016), 1610.07810.
- [10] L. Giusti and M. Pepe, Phys. Lett. **B769**, 385 (2017), 1612.00265.
- [11] K. Kanaya *et al.*, PoS **Lattice 2016**, 063 (2016), 1610.09518. M. Dalla Brida, L. Giusti, and M. Pepe, (2017), 1710.09219.
- [12] G. Boyd *et al.*, Nucl. Phys. **B469**, 419 (1996), hep-lat/9602007.
- [13] B. Lucini, M. Teper, and U. Wenger, Phys. Lett. **B545**, 197 (2002), hep-lat/0206029. B. Lucini, M. Teper, and U. Wenger, JHEP **0401**, 061 (2004), hep-lat/0307017.
- [14] B. Lucini, M. Teper, and U. Wenger, JHEP **0502**, 033 (2005), hep-lat/0502003.
- [15] F. Bursa and M. Teper, JHEP **0508**, 060 (2005), hep-lat/0505025. B. Bringoltz and M. Teper, Phys. Lett. **B628**, 113 (2005), hep-lat/0506034. B. Bringoltz and M. Teper, Phys. Rev. **D73**, 014517 (2006), hep-lat/0508021. M. Pepe and U.-J. Wiese, Nucl. Phys. **B768**, 21 (2007), hep-lat/0610076. G. Cossu, M. D’Elia, A. Di Giacomo, B. Lucini, and C. Pica, JHEP **0710**, 100 (2007), 0709.0669. T. Umeda *et al.*, Phys. Rev. **D79**, 051501 (2009), 0809.2842. H. B. Meyer, Phys. Rev. **D80**, 051502 (2009), 0905.4229.
- [16] M. Panero, PoS **Lattice 2008**, 175 (2008), 0808.1672.
- [17] M. Panero, Phys. Rev. Lett. **103**, 232001 (2009), 0907.3719. S. Datta and S. Gupta, Phys. Rev. **D80**, 114504 (2009), 0909.5591. B. H. Wellegehausen, A. Wipf, and C. Wozar, Phys. Rev. **D80**, 065028 (2009), 0907.1450. S. Datta and S. Gupta, Phys. Rev. **D82**, 114505 (2010), 1006.0938.
- [18] S. Borsányi, G. Endrődi, Z. Fodor, S. D. Katz, and K. K. Szabó, JHEP **1207**, 056 (2012), 1204.6184.
- [19] A. Mykkänen, M. Panero, and K. Rummukainen, JHEP **1205**, 069 (2012), 1202.2762.
- [20] B. Lucini, A. Rago, and E. Rinaldi, Phys. Lett. **B712**, 279 (2012), 1202.6684.
- [21] B. Lucini and M. Panero, Phys. Rept. **526**, 93 (2013), 1210.4997. FlowQCD, M. Asakawa, T. Hatsuda, E. Itou, M. Kitazawa, and H. Suzuki, Phys. Rev. **D90**, 011501 (2014), 1312.7492, [Erratum: Phys. Rev. **D92**, no.5, 059902 (2015)]. L. Giusti and M. Pepe, Phys. Rev. Lett. **113**, 031601 (2014), 1403.0360. M. Bruno, M. Caselle, M. Panero, and R. Pellegrini, JHEP **1503**, 057 (2015), 1409.8305. C. Bonati, JHEP **03**, 006 (2015), 1501.011722.

- [22] A. Francis, O. Kaczmarek, M. Laine, T. Neuhaus, and H. Ohno, Phys. Rev. **D91**, 096002 (2015), 1503.05652.
- [23] O. Hajizadeh and A. Maas, Eur. Phys. J. **A53**, 207 (2017), 1702.08724.
- [24] J. Christensen, G. Thorleifsson, P. Damgaard, and J. Wheeler, Nucl. Phys. **B374**, 225 (1992). K. Holland, JHEP **0601**, 023 (2006), hep-lat/0509041. K. Holland, M. Pepe, and U.-J. Wiese, JHEP **0802**, 041 (2008), 0712.1216. J. Liddle and M. Teper, (2008), 0803.2128. P. Bialas, L. Daniel, A. Morel, and B. Petersson, Nucl. Phys. **B807**, 547 (2009), 0807.0855. M. Caselle, L. Castagnini, A. Feo, F. Gliozzi, and M. Panero, JHEP **1106**, 142 (2011), 1105.0359. M. Caselle *et al.*, JHEP **1205**, 135 (2012), 1111.0580. P. Bialas, L. Daniel, A. Morel, and B. Petersson, Nucl. Phys. **B871**, 111 (2013), 1211.3304.
- [25] C. Jarzynski, Phys. Rev. Lett. **78**, 2690 (1997), cond-mat/9610209.
- [26] C. Jarzynski, Phys. Rev. **E56**, 5018 (1997), cond-mat/9707325.
- [27] D. J. Evans, E. G. D. Cohen, and G. P. Morriss, Phys. Rev. Lett. **71**, 2401 (1993). D. J. Evans and D. J. Searles, Phys. Rev. **E50**, 1645 (1994). G. Gallavotti and E. G. D. Cohen, Phys. Rev. Lett. **74**, 2694 (1995), chao-dyn/9410007. G. Gallavotti and E. G. D. Cohen, J. Stat. Phys. **80**, 931 (1995), chao-dyn/9501015. G. E. Crooks, J. Stat. Phys. **90**, 1481 (1998). G. E. Crooks, Phys. Rev. **E60**, 2721 (1999), cond-mat/9901352. G. E. Crooks, Phys. Rev. **E61**, 2361 (2000), cond-mat/9908420. F. Ritort, Poincaré Seminar **2**, 195 (2003), cond-mat/0401311. U. Marini Bettolo Marconi, A. Puglisi, L. Rondoni, and A. Vulpiani, Phys. Rept. **461**, 111 (2008), 0803.0719.
- [28] M. Caselle, G. Costagliola, A. Nada, M. Panero, and A. Toniato, Phys. Rev. **D94**, 034503 (2016), 1604.05544.
- [29] A. Nada, M. Caselle, and M. Panero, (2017), 1710.04435.
- [30] S. Nosé, J. Chem. Phys. **81**, 511 (1984). W. G. Hoover, Phys. Rev. **A31**, 1695 (1985).
- [31] R. M. Neal, Statistics and Computing **11**, 125 (2001).
- [32] H. Stöcker *et al.*, Journal of Physics G: Nuclear and Particle Physics **43**, 015105 (2016), 1509.00160. H. Stöcker *et al.*, Astron. Nachr. **336**, 744 (2015), 1509.07682.
- [33] P. H. Ginsparg, Nucl. Phys. **B170**, 388 (1980). T. Appelquist and R. D. Pisarski, Phys. Rev. **D23**, 2305 (1981).
- [34] S. Nadkarni, Phys. Rev. **D27**, 917 (1983). E. Braaten and R. D. Pisarski, Nucl. Phys. **B337**, 569 (1990).
- [35] E. Braaten and A. Nieto, Phys. Rev. **D53**, 3421 (1996), hep-ph/9510408.

- [36] E. Braaten and A. Nieto, Phys. Rev. **D51**, 6990 (1995), hep-ph/9501375. K. Kajantie, M. Laine, K. Rummukainen, and M. E. Shaposhnikov, Nucl. Phys. **B458**, 90 (1996), hep-ph/9508379.
- [37] K. Kajantie, M. Laine, K. Rummukainen, and Y. Schröder, Phys. Rev. **D67**, 105008 (2003), hep-ph/0211321.
- [38] A. D. Linde, Phys. Lett. **B96**, 289 (1980). D. J. Gross, R. D. Pisarski, and L. G. Yaffe, Rev. Mod. Phys. **53**, 43 (1981).
- [39] M. Creutz, Phys. Rev. **D21**, 2308 (1980). A. Kennedy and B. Pendleton, Phys. Lett. **B156**, 393 (1985).
- [40] S. L. Adler, Phys. Rev. **D23**, 2901 (1981). F. R. Brown and T. J. Woch, Phys. Rev. Lett. **58**, 2394 (1987).
- [41] J. Shao and D. Tu, *The Jackknife and Bootstrap* (Springer-Verlag, New York, 1995).
- [42] R. Sommer, Nucl. Phys. **B411**, 839 (1994), hep-lat/9310022.
- [43] S. Necco and R. Sommer, Nucl. Phys. **B622**, 328 (2002), hep-lat/0108008.
- [44] F. Karsch, E. Laermann, and A. Peikert, Phys. Lett. **B478**, 447 (2000), hep-lat/0002003.
- [45] M. Pepe, PoS **Lattice 2005**, 017 (2006), hep-lat/0510013.
- [46] C. E. DeTar, Phys. Rev. **D32**, 276 (1985). H. T. Elze, K. Kajantie, and J. I. Kapusta, Nucl. Phys. **B304**, 832 (1988). F. Gliozzi, J. Phys. **A40**, F375 (2007), hep-lat/0701020.
- [47] H. B. Meyer, JHEP **07**, 059 (2009), 0905.1663.
- [48] R. Hagedorn, Nuovo Cim. Suppl. **3**, 147 (1965).
- [49] M. Caselle, A. Nada, and M. Panero, JHEP **07**, 143 (2015), 1505.01106, [Erratum: JHEP **11**, 016 (2017)]. P. Alba, W. M. Alberico, A. Nada, M. Panero, and H. Stöcker, Phys. Rev. **D95**, 094511 (2017), 1611.05872.
- [50] E. V. Shuryak, Sov. Phys. JETP **47**, 212 (1978). S. Chin, Phys. Lett. **B78**, 552 (1978).
- [51] J. I. Kapusta, Nucl. Phys. **B148**, 461 (1979).
- [52] T. Toimela, Phys. Lett. **B124**, 407 (1983).
- [53] P. B. Arnold and C.-X. Zhai, Phys. Rev. **D50**, 7603 (1994), hep-ph/9408276. P. B. Arnold and C.-X. Zhai, Phys. Rev. **D51**, 1906 (1995), hep-ph/9410360.
- [54] C.-X. Zhai and B. M. Kastening, Phys. Rev. **D52**, 7232 (1995), hep-ph/9507380.

- [55] K. Kajantie, M. Laine, K. Rummukainen, and Y. Schröder, *JHEP* **04**, 036 (2003), hep-ph/0304048.
- [56] K. Kajantie, M. Laine, K. Rummukainen, and M. E. Shaposhnikov, *Nucl. Phys.* **B503**, 357 (1997), hep-ph/9704416.
- [57] K. Kajantie, M. Laine, K. Rummukainen, and Y. Schröder, *Phys. Rev. Lett.* **86**, 10 (2001), hep-ph/0007109. A. Hietanen, K. Kajantie, M. Laine, K. Rummukainen, and Y. Schröder, *Phys. Rev.* **D79**, 045018 (2009), 0811.4664.
- [58] S. Caron-Huot, *Phys. Rev.* **D79**, 065039 (2009), 0811.1603. M. Laine, *Eur. Phys. J.* **C72**, 2233 (2012), 1208.5707. M. Benzke, N. Brambilla, M. A. Escobedo, and A. Vairo, *JHEP* **1302**, 129 (2013), 1208.4253. M. Panero, K. Rummukainen, and A. Schäfer, *Phys. Rev. Lett.* **112**, 162001 (2014), 1307.5850. J. Ghiglieri *et al.*, *JHEP* **1305**, 010 (2013), 1302.5970. M. D’Onofrio, A. Kurkela, and G. D. Moore, *JHEP* **1403**, 125 (2014), 1401.7951.
- [59] J.-P. Blaizot, E. Iancu, and A. Rebhan, (2003), hep-ph/0303185. J. O. Andersen, E. Braaten, and M. Strickland, *Phys. Rev. Lett.* **83**, 2139 (1999), hep-ph/9902327. J. O. Andersen, E. Braaten, and M. Strickland, *Phys. Rev.* **D61**, 014017 (2000), hep-ph/9905337. J. O. Andersen, M. Strickland, and N. Su, *Phys. Rev. Lett.* **104**, 122003 (2010), 0911.0676. J. O. Andersen, L. E. Leganger, M. Strickland, and N. Su, *JHEP* **1108**, 053 (2011), 1103.2528.
- [60] J. M. Maldacena, *Adv. Theor. Math. Phys.* **2**, 231 (1998), hep-th/9711200. S. Gubser, I. R. Klebanov, and A. M. Polyakov, *Phys. Lett.* **B428**, 105 (1998), hep-th/9802109. E. Witten, *Adv. Theor. Math. Phys.* **2**, 253 (1998), hep-th/9802150.
- [61] R. D. Pisarski, *Phys. Rev.* **D62**, 111501 (2000), hep-ph/0006205. P. N. Meisinger, T. R. Miller, and M. C. Ogilvie, *Phys. Rev.* **D65**, 034009 (2002), hep-ph/0108009. K. Fukushima, *Phys. Lett.* **B591**, 277 (2004), hep-ph/0310121. A. Dumitru, Y. Hatta, J. Lenaghan, K. Orginos, and R. D. Pisarski, *Phys. Rev.* **D70**, 034511 (2004), hep-th/0311223. C. Ratti, M. A. Thaler, and W. Weise, *Phys. Rev.* **D73**, 014019 (2006), hep-ph/0506234. R. D. Pisarski, *Phys. Rev.* **D74**, 121703 (2006), hep-ph/0608242. A. Vuorinen and L. G. Yaffe, *Phys. Rev.* **D74**, 025011 (2006), hep-ph/0604100. K. Kajantie, T. Tahkokallio, and J.-T. Yee, *JHEP* **0701**, 019 (2007), hep-ph/0609254. U. Gürsoy and E. Kiritsis, *JHEP* **0802**, 032 (2008), 0707.1324. O. Andreev, *Phys. Rev.* **D76**, 087702 (2007), 0706.3120. U. Gürsoy, E. Kiritsis, L. Mazzanti, and F. Nitti, *Phys. Rev. Lett.* **101**, 181601 (2008), 0804.0899. U. Gürsoy, E. Kiritsis, L. Mazzanti, and F. Nitti, *Nucl. Phys.* **B820**, 148 (2009), 0903.2859. J. Alanen, K. Kajantie, and V. Suur-Uski, *Phys. Rev.* **D80**, 126008 (2009), 0911.2114. Y. Hidaka and R. D. Pisarski, *Phys. Rev.* **D78**, 071501 (2008), 0803.0453. K. Fukushima, *Phys. Rev.* **D77**, 114028 (2008), 0803.3318, [Erratum: *Phys. Rev.* **D78**, 039902 (2008)]. E. Megías, E. Ruiz Arriola, and L. L. Salcedo, *Phys. Rev.* **D80**, 056005 (2009), 0903.1060. A. Dumitru, Y. Guo, Y. Hidaka, C. P. K. Altes, and R. D. Pisarski, *Phys. Rev.* **D83**, 034022 (2011), 1011.3820. A. Dumitru, Y. Guo, Y. Hidaka, C. P. K. Altes, and R. D. Pisarski, *Phys. Rev.* **D86**, 105017 (2012), 1205.0137.

- [62] A. M. Ferrenberg and R. H. Swendsen, Phys. Rev. Lett. **61**, 2635 (1988). I. M. Barbour, S. E. Morrison, E. G. Klepfish, J. B. Kogut, and M.-P. Lombardo, Phys. Rev. **D56**, 7063 (1997), hep-lat/9705038. Z. Fodor and S. D. Katz, Phys. Lett. **B534**, 87 (2002), hep-lat/0104001.
- [63] A. Pohorille, C. Jarzynski, and C. Chipot, J. Phys. Chem. **B114**, 10235 (2010). N. Yunger Halpern and C. Jarzynski, Phys. Rev. **E93**, 052144 (2016), 1601.02637.
- [64] Y. Aoki *et al.*, JHEP **0906**, 088 (2009), 0903.4155. A. Bazavov *et al.*, Phys. Rev. **D85**, 054503 (2012), 1111.1710.
- [65] T. Bhattacharya *et al.*, Phys. Rev. Lett. **113**, 082001 (2014), 1402.5175. tmfT, F. Burger, E.-M. Ilgenfritz, M. P. Lombardo, and M. Müller-Preussker, Phys. Rev. **D91**, 074504 (2015), 1412.6748. Y. Taniguchi *et al.*, Phys. Rev. **D96**, 014509 (2017), 1609.01417.
- [66] M. Lüscher, P. Weisz, and U. Wolff, Nucl. Phys. **B359**, 221 (1991). M. Lüscher, R. Narayanan, P. Weisz, and U. Wolff, Nucl. Phys. **B384**, 168 (1992), hep-lat/9207009. M. Lüscher, R. Sommer, U. Wolff, and P. Weisz, Nucl. Phys. **B389**, 247 (1993), hep-lat/9207010. M. Lüscher, R. Sommer, P. Weisz, and U. Wolff, Nucl. Phys. **B413**, 481 (1994), hep-lat/9309005. S. Sint, Nucl. Phys. **B421**, 135 (1994), hep-lat/9312079. S. Sint and R. Sommer, Nucl. Phys. **B465**, 71 (1996), hep-lat/9508012. ALPHA, A. Bode, U. Wolff, and P. Weisz, Nucl. Phys. **B540**, 491 (1999), hep-lat/9809175. ALPHA, A. Bode, P. Weisz, and U. Wolff, Nucl. Phys. **B576**, 517 (2000), hep-lat/9911018, [Erratum: Nucl. Phys. **B608**, 481 (2001)].
- [67] P. V. Buividovich and M. I. Polikarpov, Phys. Lett. **B670**, 141 (2008), 0806.3376. P. V. Buividovich and M. I. Polikarpov, Nucl. Phys. **B802**, 458 (2008), 0802.4247. A. Velytsky, Phys. Rev. **D77**, 085021 (2008), 0801.4111. W. Donnelly, Phys. Rev. **D85**, 085004 (2012), 1109.0036. S. Aoki *et al.*, JHEP **06**, 187 (2015), 1502.04267. Đ. Radičević, JHEP **04**, 163 (2016), 1509.08478. E. Itou, K. Nagata, Y. Nakagawa, A. Nakamura, and V. I. Zakharov, PTEP **2016**, 061B01 (2016), 1512.01334.